Smart Pressure Sensor on SOI optimized by Finite Element Analysis for Heatspreader Integration

Bogdan Bercu, Laurent Montès*, Panagiota Morfouli
Institute of Microelectronics, Electromagnetism and Photonics (IMEP - UMR 5130 INPG-UJF-CNRS), IMEP-ENSERG/Minatec, 23 rue des martyrs, BP 247, 38016 Grenoble Cedex 1
**Email: laurent.montes@inpg.fr Phone: +33 (0)476-856-057 Fax: +33 (0)476-856-070*

ABSTRACT

In this contribution are presented the results concerning the optimization of a piezoresistive pressure sensor, integrated into a microheat-spreader entirely micromachined in silicon. The membrane limited area, imposed by the heat spreader geometry, requires the use of an ultra thin membrane. Results from FEA calculations are indicating a good sensitivity for 0.7µm membrane thickness, with a good linearity in the pressure domain of interest. The whole structure is micromachined in SOI wafers in order to provide a better sensor reproducibility across the wafer. Temperature and residual stress influences are also taken into account, a high doping level and a three-layered membrane being proposed in order to reduce the temperature dependence and the residual stress effects.

1 INTRODUCTION

Efficient temperature control is an important topic in many fields of microelectronics due to the ever-increasing heat flux generated by the electronic devices. In this context the implementation of heat spreaders is of great interest due to their compactness and to the IC technology compatibility. Complete integration of heat spreaders by micro machining of Si wafers and molecular wafer bonding has been reported [1]. Tests carried out on several specific designs are showing their considerable improvement with respect to thermal conductivity (up to 10 times the thermal conductivity of Si bulk [2]). The modeling background for optimizing a specific spreader design is also available [3, 4], although it needs further testing for specific applications. In this context internal pressure, temperature and flow sensors are vital assets to this kind of study in order to reach an optimal configuration that will allow a maximized dissipated heat flux for a maximized compactness.

The piezoresistive pressure sensors micro machined on SOI wafers [5] are an option of choice due to the fact that the layer of buried oxide allows to stop the etching process with a high accuracy. One can obtain in this way ultra thin membranes (total thickness lower than 1µm), highly homogeneous and reproducible. The use of such thin membranes concerns the applications were their area is limited (lateral size in the order of 100-200µm), the sensitivity of the sensor being critically dependent on the membrane thickness.

Several parameters, such as the lateral membrane size and the operating pressure domain, have been chosen to follow a specific heat spreader design. In this contribution we present the results obtained by FEA calculations concerning the optimization of the sensor response to the applied pressure. Several parameters have been optimized, such as the membrane thickness, the positioning of the piezoresistive gauges on the membrane and the geometry of the piezoresistive gauges.

2 INTEGRATION OF PIEZORESISTIVE PRESSURE SENSORS

The working principle of the chosen type of heat spreader is schematically presented in Figure 1. The cavity is filled with a liquid (water, alcohol, etc), the vapors produced in the proximity of the heat source flowing towards the cooled walls where they condense, thus insuring the heat transport [2]. The capillary wick assures the pumping of the condensed liquid back to the heated zone by the pressure drop between the hot and the cold ends of the channels (difference in the filling liquid radius in the channel).

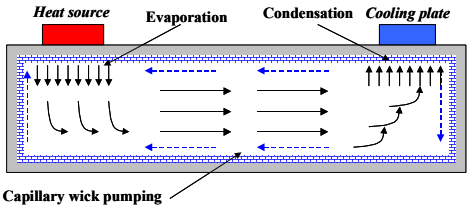

Fig 1 *Working principle of the vapor chamber heat spreader.*

The choice for using piezoresistive pressure sensors is mainly due to their relatively straightforward technological implementation and robustness [6]. Its integration into the technological process, as presented in Figure 2, adds only a single additional step of deep Si etching, which correspond to the sensors membrane micromachining.

The process, which remains totally IC compatible, is composed of two main parts: **a)** patterning of the sensitive elements (stress gauges) and of the contacts on the top SOI layer (CMOS standard technology) and **b)** micromachining

by deep reactive plasma etch on the backside of the wafer of the vapor chamber, the capillary network (longitudinal channels) and pressure sensor membranes (Fig. 3).

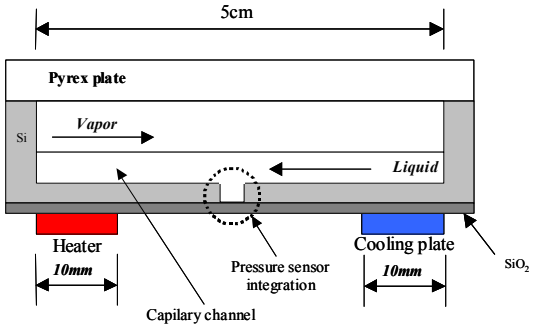

Fig. 2. *Heat spreader schematic longitudinal cut, showing the integration solution for pressure sensors.*

The choice of this original three-step etch process on one wafer is to be able to seal the vapor chamber (Fig. 2) either with pyrex plate (for microfluidics test measurements), or with a second Si wafer, previously wick patterned (for producing the heat spreader).

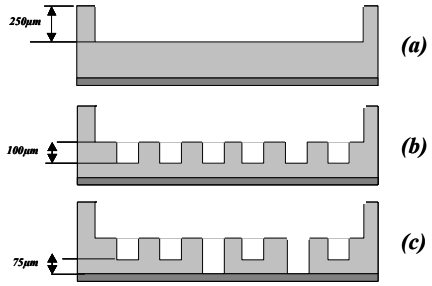

Fig. 3. *Illustration of the three-step micromachining process:* ***(a)*** *vapor chamber,* ***(b)*** *capillary wick and* ***(c)*** *membrane micromachining.*

As shown in Fig. 3, the pressure sensor membrane is micromachined in the heat spreader wall in order to be able to measure accurately the pressure inside the cavity. Therefore the membrane size is dependent on the channel width, which in return has to be optimized in order to assure an efficient liquid pumping [4]. For the specific heat spreader dimensions– vapor cavity of 5cm in length, 1cm in width and 250µm in height, a value of 160µm is found as the channel width optimum for a maximal heat flux transfer (using water as working fluid).

The sensitive elements are piezo-resistors – doped regions in crystalline Si (Fig. 4), connected in a Wheatstone bridge configuration. When a pressure is applied on the membrane, the in-plane stress modifies the carrier mobility, changing the electrical resistance of the gauges and therefore producing a nonzero output voltage at the bridge output [6].

The resulting relative resistance variation of each individual stress gauge as a function of the in-plane mechanical stress is given by [7]:

$$\frac{\Delta R}{R} = \pi_l \sigma_l + \pi_t \sigma_t \qquad (1)$$

where π_l et π_t are the longitudinal and transversal piezoresistive coefficients and σ_l and σ_t are the longitudinal and transversal components of the mechanical stress in the membrane, relative to the current flow direction. The piezoresistive coefficients are depending on doping type and concentration, temperature and crystalline orientation [7, 8].

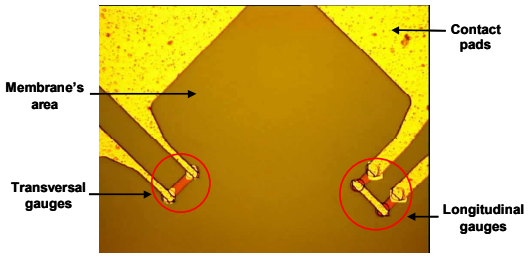

Fig. 4 *Top view of the fabricated sensors, showing the stress gauges and the contact pads.*

For a p-type doping the maximal resistance variation is obtained when the current flows parallel to <110> crystalline directions, the longitudinal and transversal piezoresistive coefficients being given by:

$$\pi_l = \frac{1}{2}\left(\pi_{11} + \pi_{12} + \pi_{44}\right) \qquad (2)$$

$$\pi_t = \frac{1}{2}\left(\pi_{11} + \pi_{12} - \pi_{44}\right) \qquad (3)$$

where π_{11}, π_{12} and π_{44} are the linear piezoresistive coefficients, characteristics to the doped material for a given temperature and doping level [7, 8]. For an n-type doping the maximal piezoresistive effect is obtained when the current flows parallel to <100> crystalline directions, the longitudinal and transversal coefficients being given by:

$$\pi_l = \pi_{11}; \quad \pi_t = \pi_{12} \qquad (4)$$

In our case, each longitudinal stress gauge has been divided in two equal and parallel parts (Fig. 1) in order to increase their sensitivity (the stress distribution along the length is more homogenous for shorter gauges).

3 RESULTS AND DISCUSSION

In order to optimize the sensor configuration for obtaining a maximized sensitivity, we have performed a series of FEA concerning its response to the applied pressure (Fig. 5) as a function of several parameters, such as the membrane thickness, the dimensions of the resistors and their position on the membrane, doping type, etc. The bulk meshing has been refined near the membrane edges.

As we intend to use a SOI wafer in order to have a good control over the etch depth, the sensor membrane will consist of two layers: SiO_2 and crystalline Si. In addition, an extra layer of thermal grown SiO_2 can be added on top of

the structure in order to reduce the effects of the residual stress [9].

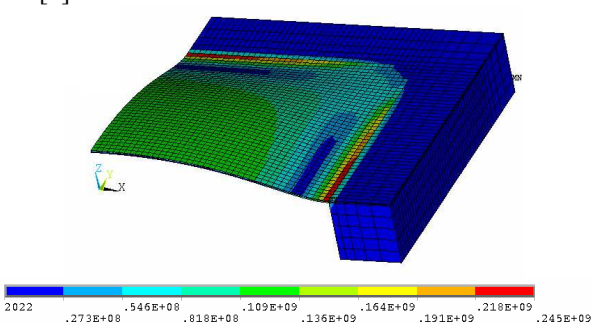

Fig. 5 *3D stress distribution on the deformed membrane for a 50kPa applied pressure (scale in Pa).*

The membrane thickness is a key factor for the overall response, in correlation with the lateral dimensions. In Fig. 6 one can observe the considerable increase of the gauge simulated response with the decrease in thickness of the Si layer (values calculated for a fixed thickness of 0.4µm for the SiO_2 layer).

An important limiting factor concerning the thickness is the maximal operational pressure (burst pressure) [6]:

$$P_{\text{limit}} = 3.25\sigma_{\max}\left(\frac{h}{L}\right)^2 \qquad (5)$$

where σ_{max} is the rupture stress. Considering the internal pressure domain of the heat spreader in the range of 150kPa, we have chosen a total membrane thickness of 0.7µm (0.4µm of SiO_2 and 0.3µm of Si), which leads to an operation pressure limit of roughly 500kPa (the value of the maximal stress in Si being estimated to 7GPa [6]).

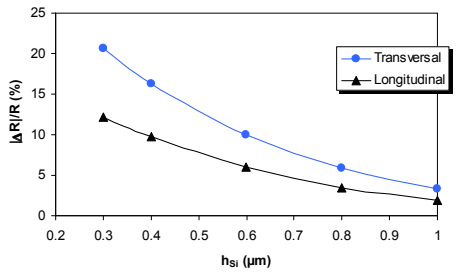

Fig. 6 Relative variation of the gauge resistance as a function of Si thickness (0.4µm SiO_2 thickness, P=50kPa).

A critical parameter for the sensors performance is the gauge positioning on the membrane, the maximal change in resistance being achieved around the maxima of the in-plane stress. As we intend to use (100) orientated wafers, we have investigated both types of gauge configurations: p-type resistors, orientated along the <110> crystalline direction, and n-type resistors, orientated along the <100> crystalline direction.

Considering a set of p-type gauges, at a concentration of $4.6x10^{16}$at/cm^3, of 10µm in length and 4µm in width, the resistance variation for 50kPa of applied pressure shows a pronounced maximum around 16µm (Fig. 7). The resistance variation is considerable: 12% for the longitudinal and 20% for the transversal gauge (compared to 1.5% for a 2µm thick membrane of identical side size). The maximal membrane deflection (1.9µm) is also considerable. The deflection resulting from the residual stress was found to be relatively small (3.4nm) for the given membrane dimensions and therefore negligible.

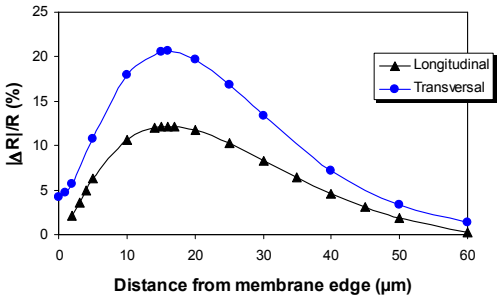

Fig. 7 *Relative resistance variation of gauge versus positioning (p-type doping).*

In this configuration the gauges response as a function of the applied pressure is quasi-linear in the 10 to 50kPa pressure domain (standard error of estimate: $(\sigma_{est})_T$=0.25% and $(\sigma_{est})_L$=0.18%).

The optimal position for gauge placement on the membrane remains unchanged when using n-type resistors, the response dependence as a function of position being similar to the one for the p-doped gauges, with different maximal values.

The relative resistance variation of the gauges as a function of their geometry (length, width and spacing between the components of each pair of longitudinal gauges) was also investigated in order to further optimize the sensor response (L=10µm, W=4µm and t=5µm).

The output voltage of the sensor as a function of the applied pressure was simulated for both configurations, using the optimal gauge parameters (Fig. 8). The use of n-type stress gauges leads to a 20% improvement of sensitivity (up to a value of 1.4mV/kPa) compared to the p-type stress gauges. One can notice again the good linearity of the sensor response: $(\sigma_{est})_{p\text{-type}}$=0.74mV and $(\sigma_{est})_{n\text{-type}}$=0.63mV.

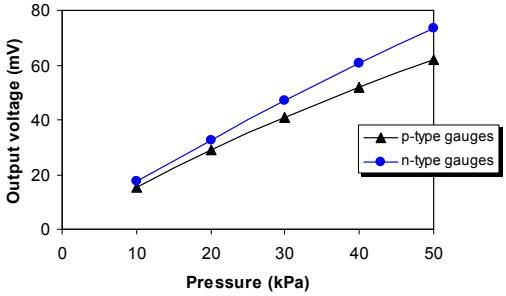

Fig. 8 *Output voltage for 1V of applied tension (T=27°C, C=$4.6x10^{16}$at/cm^3).*

Considering the temperature variations along the heat spreader length, the sensor response was simulated for a temperature range of 25 to 80°C, for several doping levels. The choice for a higher doping level is made in order to reduce the temperature sensitivity of the sensor, thus insuring a higher reliability of the measurements. A reduction of 30% of sensor sensitivity variation with temperature (in 25-80°C range) is achieved by using highly doped gauges ($C=9x10^{18}cm^{-3}$). The pressure sensitivity for the higher doping level is satisfactory: $S_{average}=0.85mV/kPa$, the linearity in response being maintained ($(\sigma_{est})_{27°C}=1.15mV$ and $(\sigma_{est})_{80°C}=2.44mV$).

In order to reduce the effects of the residual stress in the membrane behavior, we have investigated a three-layered membrane: 400nm SiO_2/300nm Si/400nm SiO_2 (Fig. 9), the second SiO_2 layer being obtained by thermal oxidation of the SOI layer.

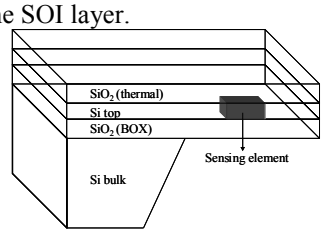

Fig. 9 *Scheme of the three-layered sensor membrane.*

Using the same previous optimal parameters for stress gauges geometry, doping type and dopant level, the optimal gauge position on the membrane is placed at 22.5µm from the membrane edge.

As we can see from Fig. 10, the sensor sensitivity is slightly decreased: $S_{average}=0.55mV/kPa$, the linearity in sensor response being improved: $(\sigma_{est})_{average}=0.06mV$.

The first prototype of the heat spreader with integrated sensors was achieved, its characterization being currently in progress.

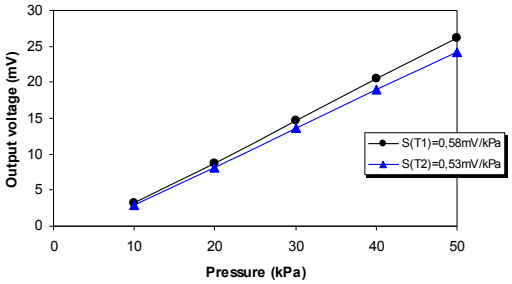

Fig. 10. *Sensor response for the three-layered structure ($C=9x10^{18}at/cm^3$; $T_1=27°C$, $T_2=80°C$).*

4 CONCLUSIONS

In this contribution we present the results obtained by FEA calculations concerning the response enhancement for a piezoresistive pressure sensor with a relatively small membrane area (150x150µm²). The use of an ultra-thin membrane (0.7µm - 400nm SiO_2/300nm Si), micromachined in a SOI wafer, reveals a considerable increase in the sensor response. The optimal gauge dimensions have been determined (L=10µm and W=4µm), as well as the optimal gauge positioning on the membrane (16µm from membranes edge), for the pressure domain of interest (10kPa to 50kPa).

Higher sensor output was found to by provided by the n-doped gauges, orientated along <100> crystalline directions. The response of the optimized sensor is quasi-linear for the specified pressure domain. Highly doped gauges ($10^{19}at/cm^3$) are to be used due to their lower sensitivity with temperature (8% of pressure sensitivity variation in the 25-80°C domain).

An important increase in sensor response linearity has been has been achieved by using a three-layered membrane. It provides a significantly lower residual stress, with an average sensitivity of 0.55mV/kPa and $\sigma_{est}=0.06mV$ for the above mentioned parameters.

ACKNOWLEDGEMENTS

The authors would like to thank to the Région Rhône-Alpes for the financial support granted to this project.

REFERENCES

[1] M. Le Berre, S. Launay, V. Sartre, M. Lallemand, "Fabrication and experimental investigation of silicon micro heat pipes for cooling electronics", J. of Micromech. and Microeng., Vol. 13 (2003), pp. 436-441.

[2] A. Lai, C. Gillot, M. Ivanova, Y. Avenas, C. Louis, C. Schaeffer, E. Fournier, "Thermal Characterization of Flat Silicon Heat Pipes", *Proc 22th Annual IEEE Semiconductor Thermal Measurement and Management Symposium,* March 2004, pp. 21-25

[3] T. Q. Feng, J. L. Xu, "An analytical solution of thermal resistance of cubic heat spreaders for electronic cooling", *Appl. Therm. Eng.*, Vol. 24 (2004), pp. 323–337.

[4] S. Tzanova, M. Ivanova, Y. Avenas, Ch. Schaeffer, "Analytical Investigation of Flat Silicon Micro Heat Spreaders", *Proc. 2004 IEEE Industry Applications Conf. - 39th IAS Annual Meeting*, October 2004, pp. 2296-2302 (Vol. 4)

[5] S. Renard, "Industrial MEMS on SOI", *J. Micromech. Microeng.*, Vol. 10 (2000), pp. 245–249

[6] G. Blasquez, P. Pons, A. Eoukabache, "Capabilities and limits of silicon pressure sensors", *Sensor. Actuator. Phys.*, Vol. 17 (1989), pp. 387-404.

[7] C. S. Smith, "Piezoresistance Effect in Germanium and Silicon", *Phys. Rev.*, Vol. 94, No. 1 (1954), pp. 42-49.

[8] O. N. Tufte, E. L. Stelzer, "Piezoresistive Properties of Heavily Doped n-Type Silicon", *Phys. Rev.*, Vol. 133 (1963), pp. 1705-1716.

[9] J. Albert Chiou, "Simulations for Thermal Warpage and Pressure Nonlinearity of Monolithic CMOS Pressure Sensors", *IEEE Trans. Adv. Packag.*, Vol. 26, No. 3 (2003), pp. 327-333